1 INTRODUCTION

1.1 The Fischer-Tropsch synthesis history

The history of the Fischer-Tropsch Synthesis dates back to 1902 when Sabatier and Senderens synthesized methane from hydrogen and carbon monoxide for the first time. They used reduced nickel, and later cobalt, as catalysts /1/.

In 1923 Franz Fischer and Hans Tropsch at the Kaiser Wilhelm Institut fur Kohlenforschung, Mulheimruhr in Germany presented a product called "synthol". It was an oily liquid with just a small part of hydrocarbons, produced at high pressures and temperatures over alkalized iron turnings. The German industry wanted synthetic gasoline and motor fuel, and the research was turned towards catalysts and processes that mainly gave olefinic and paraffinic hydrocarbons.

The first catalyst that produced higher hydrocarbons at atmospheric pressure was reported by Franz Fischer in 1925. This catalyst contained iron oxide and zinc oxide, but later Fischer found that a mixture of cobalt oxide and chromic oxide was somewhat more active. Nickel was also found to be an interesting and active component for this purpose. The researchers experienced that the use of a catalyst support, mainly kieselguhr, and alkali and thorium promotion increased the stability and activity of the catalysts.

In 1935 Ruhrchemie started the first pilot-plant. The standard catalyst in this, and other commercial plants built during the next years, contained a mixture of Co, ThO_2, MgO and Kieselguhr.

These fuel-plants were of great importance to Germany during the second world war, but after the war many plants were destroyed, the prices of crude oil decreased, and the Fischer-Tropsch process became uneconomical. As a consequence of the price drop, plans for new plants in many countries were not realized. Only in South Africa there has been a continuous production of synthetic fuel from coal since the 1950's.

1.2 Fischer-Tropsch synthesis today

The oil crisis in 1973 led to a jump in the crude oil prices, and this in turn led to renewed interest for the Fischer-Tropsch process as a way to convert natural gas and coal to liquid fuel. Today the research is systematically directed towards three main aspects: Catalysts, reactor design and process development.

In the last twenty years new techniques and methods for investigation of catalyst surfaces have been developed. This is of great importance for getting better knowledge of the catalyst properties and structure-function relationships. Much work has been done on fundamental investigations, but still there is a lot to do before the mechanisms of the reactions are fully understood. Together with more sophisticated preparation procedures, a better understanding of the mechanisms will make it easier to design catalysts that fit our wishes better with regard to activity and selectivity.

The hydrocarbon selectivity in steady state Fischer-Tropsch synthesis is governed by Anderson-Schulz-Flory (ASF) polymerization kinetics /55/. This limits the maximum selectivity of hydrocarbons. Attempts have been done to circumvent the ASF product distribution through the use of promoters, reacting supports and combination with other catalysts. It has been shown /96/ that it is possible to increase the gasoline yield by combination with e.g. shape selective zeolites. However, there are problems connected to the quality of the gasoline, and since zeolites and the Fischer-Tropsch component generally have different optimum temperature, difficulties are also connected to the operating conditions /94/.

Because of these problems, the interest and the efforts have been focused at the production of straight-chain waxes, which is possible to achieve in high yields (close to 100 %) without breaking the AFS distribution. These products can in a second step be hydrocracked under mild conditions to a middle distillate containing jet fuel kerosine and diesel gas oil /43,93,94/. The diesel-fuel produced in this way has a high quality, being essentially sulphur- and aromatics-free and with a high cetane number.

The theoretical H_2/CO consumption ratio in the primary Fischer-Tropsch synthesis is close to 2/1. But the water gas shift reaction does also occur to some extent on all Fischer Tropsch catalysts. This will contribute to a lower H_2/CO consumption ratio. Iron catalysts show high water gas shift activity, and is preferred when synthesis gas from coal with a low H_2/CO ratio is used. When syngas is produced from hydrogen rich natural gas it has a H_2/CO ratio = 2/1 - 3/1. Cobalt and ruthenium catalysts have low water gas shift activity. Cobalt is by far the cheapest of these two metals, and therefore the most interesting when the raw material is natural gas. Nickel catalysts are not suitable in this connection because of the high methane selectivity.

The new catalysts under commercial development usually consist of four parts: A primary metal (cobalt), a secondary metal (usually noble), an oxide promoter and a support /92/.

When distillates and wax are the desired products the fluidized-bed reactor is not suitable due to wax formation on the catalyst particles, leading to defluidization of the bed /97/. Fixed-bed and slurry reactors are therefore the best choice to the production of heavy hydrocarbons.

The slurry reactor has good heat transfer conditions. This allows a simpler reactor construction, and eliminates the need for low conversion and high recycle ratio which are necessary for the fixed bed reactor. Because of this, it is supposed to have the lowest investment and operation costs /99/. Another advantageous factor of the slurry reactor is higher reaction rates due to higher operating temperature, without loss of selectivity. The slurry reactor is assumed to operate with continuous catalyst addition/removal and a problem could be to separate the catalyst from the products /93/. This can be handled in a more practical way with fixed-bed reactors. Another factor in favour of the fixed bed reactor is the vast experience and the well proven technology of this reactor type.

1.3 Background and objectives of the present work

Recently there has been reported bimetallic cobalt Fischer-Tropsch catalysts which are claimed to increase the rate of CO hydrogenation compared to monometallic cobalt catalysts. Various companies have patented different bimetallic systems with different supports (Shell: $CoZr/SiO_2$, Exxon: $CoRe/TiO_2$, Gulf: $CoRu/Al_2O_3$, Statoil: $CoRe/Al_2O_3$) /129,130,131,132/. However, very little has been published in the scientific literature about these systems and how the second metal affect the CO hydrogenation over cobalt.

The main aim of the present work has therefore been to study in what way the addition of a second metal (most of them not active for Fischer-Tropsch synthesis) influences the CO hydrogenation rate over cobalt catalysts.

The reduction behavior of mono- and bimetallic catalysts after varying pretreatment procedures has been studied, mainly by temperature programmed reduction. The available metal surface after reduction was measured by hydrogen and carbon monoxide adsorption by the volumetric method. Kinetic experiments in a fixed bed microreactor were performed in order to determine the activity and selectivity properties of the catalysts.

The work has been limited to catalysts with a fixed amount of cobalt (9 wt%) on an alumina support. Several promoting metals were used, but most of the work was done with platinum and rhenium. The effect of promoter amount and promoter precursor were studied. In addition the effect of different calcination temperatures was investigated.

The results from the study are up to now presented at the following meetings:

- the 4th Nordic Symposium on Catalysis in Trondheim, Norway, 1991: "Hydrogenation of CO over Supported Cobalt Catalysts.", oral presentation /145/.
- the 10th International Congress on Catalysis, Budapest, Hungary, 1992: "The Effect of Metallic Promoters on Supported Cobalt Catalysts", poster /146/.
- the 13th North American meeting of the Catalysis Society, Pittsburg, USA, 1993: "Study of Pt-Promoted Cobalt Fischer-Tropsch Catalysts", poster /119/.

- Europacat-I, Montpellier, France, 1993: "Hydrogenation of CO by Supported Cobalt Catalysts Promoted by Noble Metals" oral presentation /144/.

1.4 SPUNG

This work is a part of SPUNG: The State R&D Program for Utilization of Natural Gas. SPUNG's main goal is to contribute to optimal utilization of the natural gas from the Norwegian Continental Shelf through a concerted effort of research environments and industry.

Norway possesses large gas reserves - about 50 % of the known reserves in Western Europe. In addition Norway covers more than 80 % of the new proven gas reserves. With the present production level these reserves will last for more than 120 years, while the known oil reserves may be empty in about 30 to 40 years /100/.

Natural gas can be utilized in several ways. The selection of main research areas in SPUNG has been influenced by the fact that Norways gas reserves are located far from the market. The program board therefore has given priority to these three main programs:

- Chemical conversion
- Gas energy utilization
- Liquified natural gas (LNG)

The chemical conversion program has activities in catalysis, reactor technology, separation technology, and semitechnical system analysis. This work is part of the subproject catalysis.

This major research program started up in 1987. The first phase of the SPUNG program is planned to run for a period of seven years. The government funding is granted by the Ministry of Industry and the Ministry of Petroleum and Energy, and certain parts of the program are also funded by Norwegian industry.

2 LITERATURE REVIEW

2.1 Fischer Tropsch reaction mechanism

Within conversion of synthesis gas to hydrocarbons it is convenient to distinguish between methanation and the Fischer-Tropsch process /98/. Typical products from the latter are a mixture of predominantly linear alkanes and alkenes. Alcohols, usually produced in small amounts, are predominantly primary n-alcohols. Conversion to these products can be described by the following equations:

alkenes	$n\ CO + 2n\ H_2$	$\rightarrow\ C_nH_{2n} + n\ H_2O$	(n = 2,3,..)
alkanes	$m\ CO + (2m + 1)\ H_2$	$\rightarrow\ C_mH_{2m+2} + m\ H_2O$	(m = 1,2,3,..)
alcohols	$p\ CO + 2p\ H_2$	$\rightarrow\ C_{p-1}H_{2p-1}CH_2OH + (p - 1)\ H_2O$	(p = 1,2,3,..)

The literature /29,33,38,45/ shows that there is still some uncertainity about the mechanism for CO hydrogenation. But the molecular weight distribution of hydrocarbon products with three or more carbon atoms follows the Anderson-Schulz-Flory (ASF) kinetics /55/, and thus can be described by a polymerization mechanism. Methane is produced to higher extent than predicted by AFS kinetics, and ethane and ethene are produced to a lower extent /55/. The average chain length is determined by the ability of a catalyst to catalyze chain propagation versus chain termination steps. A mathematical analysis of the ASF kinetics gives the following equation:

$$\frac{W_n}{n} = (1-\alpha)^2 \cdot \alpha^{n-1} \qquad (2\text{-}1)$$

$$\alpha = \frac{r_p}{r_p + r_t} \qquad (2\text{-}2)$$

where α - the chain growth probability
n - the number of carbon atoms in the product
W_n - the weight fraction of product containing n carbon atoms
r_p - the chain propagation rate
r_t - the chain termination rate.

The logarithmic form of equation (1) is:

$$\ln \frac{W_n}{n} = \ln (1-\alpha)^2 + (n-1) \ln \alpha \qquad (2\text{-}3)$$

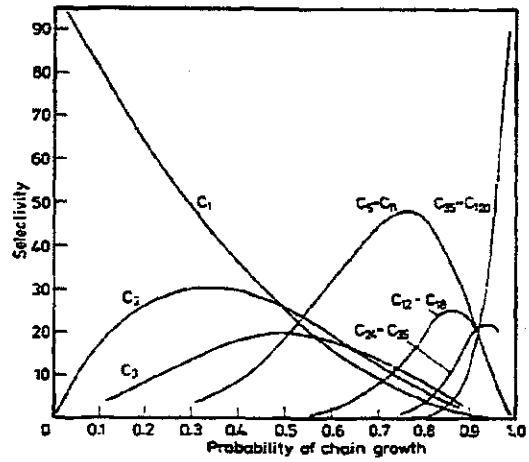

Figure 2-1. Product distribution of CO hydrogenation following ASF kinetic, vs. chain growth probability. From Dry /55/.

A least squares linear regression of ln (W_n/n) against n will give an estimate of α. Figure 2-1 /55/ shows how the theoretical product distribution of hydrocarbons depends on α, and from the figure it is obvious that methane and long chain waxes are the only products that can be produced to 100 % selectivity.

Through the years the nature of the "monomeric" unit taking part in the chain growth, and how it is formed, has been discussed. Three main types of mechanisms have been suggested:

- The surface carbide mechanism.
- The hydroxycarbene mechanism.
- The carbonyl insertion mechanism.

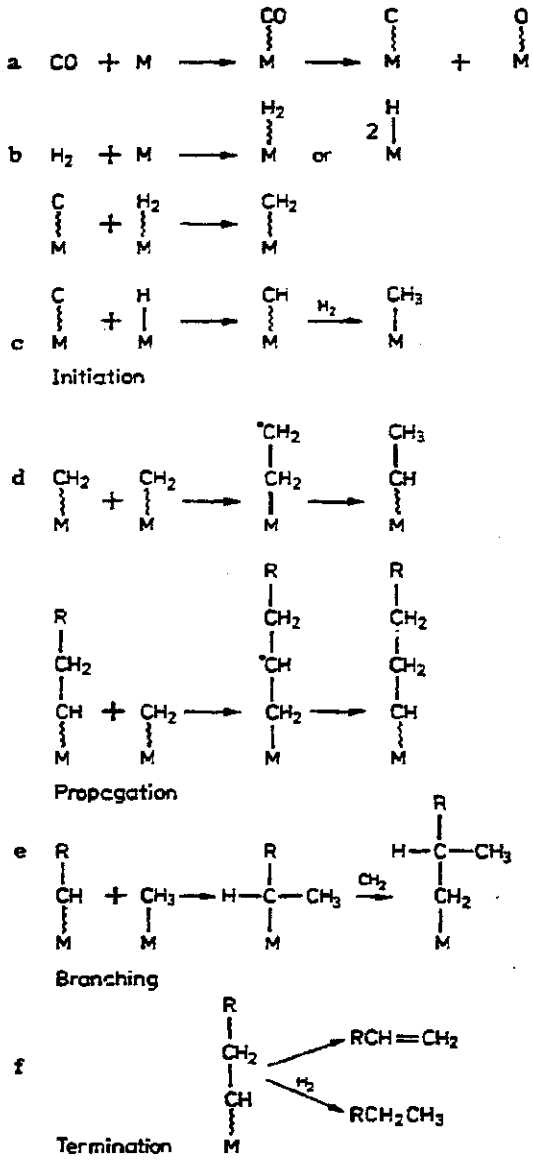

Figure 2-2. Reaction scheme for the surface carbide mechanism. From Dry /55/.

The currently most accepted mechanism is the surface carbide mechanism, shown in Figure 2-2. The assumptions for this mechanism /55/ are that CO is dissociatively adsorbed into carbon and oxygen atoms (step a). Hydrogen is chemisorbed associatively or dissociatively (step b). The carbon atoms are individually hydrogenated to CH_x species (step c). Propagation occurs by the CH_2 units linking with neighboring surface units (step d). Branching can occur by the addition of CH_3 units to the chain as in step e. Chain termination occurs by desorption, which yields the olefin, or by hydrogenation which yields the paraffin (step f). The surface carbide mechanism is a variation of the originally proposed mechanism by Fischer and Tropsch, and it has received strong support from studies involving isotopic labelling /56,98/. A weakness of the mechanism is that it does not account for the production of oxygenates without modifications. A possible way to explain oxygenate formation can be to combine the surface carbide mechanism with the carbonyl insertion mechanism, where CO is adsorbed associatively and inserts into either M-H or M-C bonds, where M represents a catalyst surface site. The question is whether the alternative schemes are really different or if they are simply variations of the same mechanism /134/. Therefore it has been attempted to present a unifying general reaction scheme. Figure 2-3 /55/ shows such a general reaction scheme which has features from both the surface carbide mechanism and the CO insertion mechanism. CO chemisorbs and becomes activated (steps a and b).The activated complex can dissociate into separate C and O atoms (step c). The C atoms are either hydrogenated to CH_2 or they migrate away to form aggregates of carbon. Alternatively the active C-O complex can be hydrogenated to form an activated CH_2O complex (A). This complex can be hydrogenated to either CH_3OH or to CH_2 and H_2O. Chain growth occurs by the reaction (e.g. insertion) of the activated C-O with hydrocarbon entities as depicted, followed by hydrogenation. Termination occurs by either desorption or hydrogenation of the oxygen-associated surface complex (B). An alternative route to acid formation via CO_2 insertion /55,28/ has been proposed.

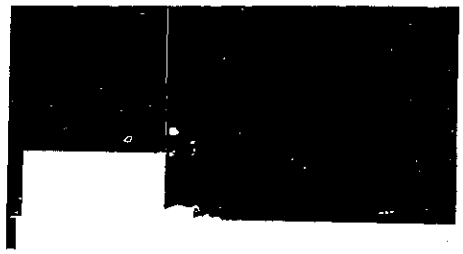

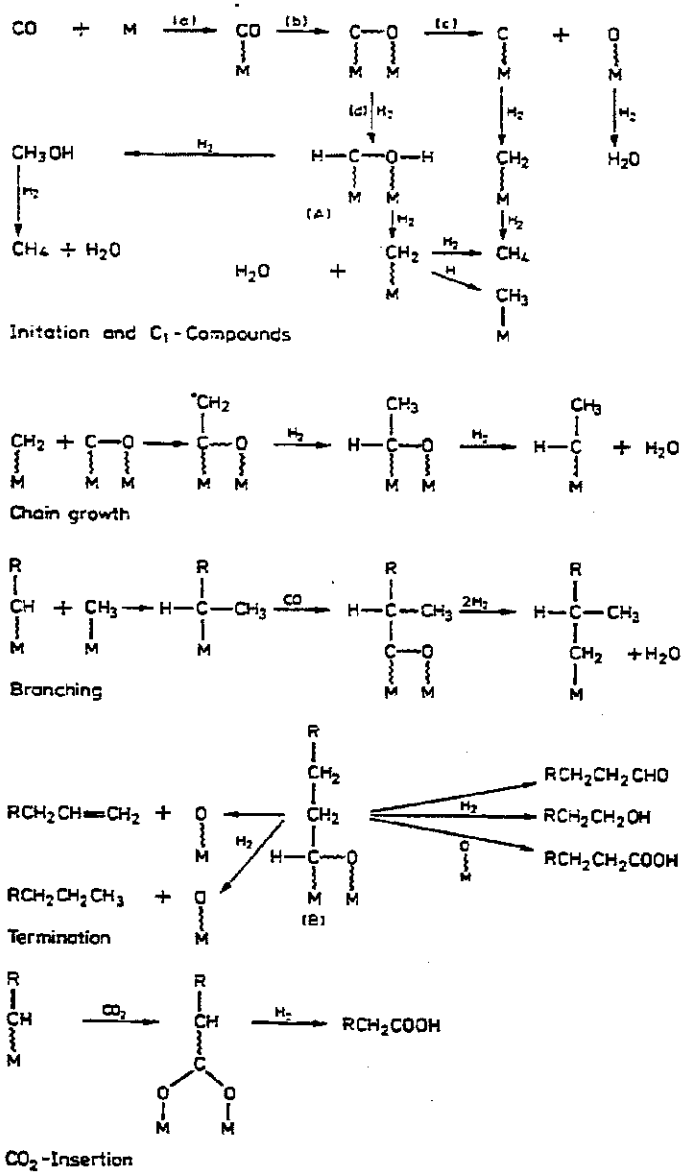

Figure 2-3. A general reaction scheme which has features from both the surface carbide mechanism and the CO insertion mechanism. From Dry /55/.

2.2 Kinetics

Langmuir-Hinschelwood type rate expressions can be derived from the different reaction mechanisms /90/. The surface carbide mechanism will here be used as an example, and after making several assumptions a general rate expression will appear. Derivations of rate expressions from other mechanisms are shown in detail elsewhere /91/.

Both hydrogen and CO are considered to be dissociatively adsorbed. All the hydrogen, carbon and oxygen atoms are assumed to be in equilibrium with their parent gas phase. The rate limiting step is supposed to be the reaction between the adsorbed surface species. The steps which appear after the rate limiting step are kinetically not important. The elementary steps of the reaction will be /90/:

$$CO\ (g) + 2* \overset{K_C}{\rightleftharpoons} C* + O* \tag{2-4}$$

$$H_2 + 2* \overset{K_H}{\rightleftharpoons} 2\ H* \tag{2-5}$$

$$C* + H* \overset{K_{C1}}{-} HC* + * \tag{2-6}$$

$$HC* + H* \overset{K_{C2}}{-} H_2C* + * \tag{2-7}$$

$$O* + H* \overset{K_{O1}}{-} HO* + * \tag{2-8}$$

$$HO* + H* \overset{K_{O2}}{-} H_2O* + 2\ * \tag{2-9}$$

The step described by eq. (6) is assumed to be the rate limiting step. The observed rate can then be expressed as:

$$-r_{CO} = k_{C1}\,[H*][C*] \tag{2-10}$$

At the same time as an adsorbed carbon atom is removed by forming HC*, an adsorbed oxygen atom must be removed from the surface. Then at steady state the two rates are equal:

$$k_{C1}\,[H*][C*] = k_{O1}\,[H*][O*] \tag{2-11}$$

The surface concentrations of hydrogen, carbon and oxygen can then be written as:

$$[H*] = K_H^{1/2}\,p_{H_2}^{1/2}\,[*] \tag{2-12}$$

$$[C*][O*] = K_C\,p_{CO}\,[*]^2 \tag{2-13}$$

$$[O*] = \frac{k_{C1}}{k_{O1}}\,[C*] \tag{2-14}$$

$$[C*] = \left(\frac{K_C\,k_{O1}}{k_{C1}}\right)^{1/2} p_{CO}^{1/2}\,[*] \tag{2-15}$$

An expression for the concentration of empty sites, [*], is found by assuming that the important surface species are adsorbed hydrogen atoms, adsorbed carbon atoms and adsorbed oxygen atoms. Then we have:

$$[*] = [*]_{tot} - [H*] - [C*] - [O*] \tag{2-16}$$

Substituting for the various known concentrations, and using Eq. (2-10) gives this rate expression for the consumption of CO:

$$-r_{CO} = \frac{(k_{C1}k_{O1}K_CK_H)^{1/2}\,p_{H_2}^{1/2}\,p_{CO}^{1/2}}{\left[1 + K_H^{1/2}\,p_{H_2}^{1/2} + \left(1 + \frac{k_{C1}}{k_{O1}}\right)\left(\frac{K_C\,k_{O1}}{k_{C1}}\right)^{1/2} p_{CO}^{1/2}\right]^2}\,[*]_{tot}^{\,2} \tag{2-17}$$

which is on the form:

$$-r_{CO} = \frac{K_1 \, p_{CO}^{1/2} \, p_{H_2}^{1/2}}{(1 + K_2 \, p_{H_2}^{1/2} + K_3 \, p_{CO}^{1/2})^2} \qquad (2\text{-}18)$$

As shown from this example, many complex rate expressions can be formulated from the different mechanisms and assumptions. None of these expressions is universally applicable to CO hydrogenation reactions. But by inserting experimental data in derivations like this, it could be a help to find possible reaction routes and to exclude those which are unpossible.

In practice it is often found /31/34/ a positive order in H_2 and a zero or negative order in CO. Kinetic data from some studies done with cobalt catalysts are shown in Table 2-1. The rate expression used is:

$$N_{CO} = A \, e^{-Ea_{CO}/RT} p_{CO}^{X} \, p_{H_2}^{Y} \qquad (2\text{-}19)$$

Table 2-1. Kinetic investigations.

Catalyst	T_{red}	T/P[a]	Ea_{CO}[b]	Ea_{CH_4}[c]	X[d]	Y[e]	N_{CO}/N_{CH_4}[f]	Ref.
3%Co/Al_2O_3	648	473-523/1	86				2.2/-	Liu /32/
10%Co/Al_2O_3	648	473-518/1	99				8.7/-	
15%Co/Al_2O_3	648	443-488/1	115				14.1/-	
2%Co/Al_2O_3	723	513-553/1	112	113	-0.5	1.2	28/20	Vannice /31/
3%Co/Al_2O_3	648	473-523/1	112				1.4/-	Fu, Bart-
10%Co/Al_2O_3	648	473-523/1	115				9.1/-	holomew
15%Co/Al_2O_3	648	473-523/1	130				11.2/-	/33/
14%Co/1%La_2O_3 on Al_2O_3	623[g]	488/8.2			-0.33	0.55		Pannel et al. /34/
3%Co/Al_2O_3	673	498-548/1	96	137			2.8/0.8	Reuel,Bart
10%Co/Al_2O_3	673	448-498/1	98	143			12.0/3.8	-holomew
15%Co/Al_2O_3	673	448-488/1	146	295				/30/

[a] Reaction temperature (K) / reaction pressure (bara).
[b] Activation energy for CO conversion, kJ/mol
[c] Activation energy for methane formation, kJ/mol
[d] Reaction order in CO
[e] Reaction order in H_2
[f] Turnover frequency for CO conversion / CH_4 formation, both given as $s^{-1} * 10^3$
[g] Reduced at 8 bara, all others at 1 bara.

2.3 Cobalt catalysis.

Cobalt catalyst systems have been used over a wide range of reaction types /65,102/. The so-called cobalt molybdate catalysts have been used extensively in the petroleum industry for hydrotreating and hydrodesulfurization. Later, these catalysts have been employed in coal liquefaction and synthoil upgrading /103/. Selective production of alcohols /143/ and oxygenate formation, as well as Fischer-Tropsch synthesis, are processes based on synthesis gas where cobalt is an important component in the catalyst system. Another field making use of cobalt catalysts is in hydrogenation of grease and oils.

Some of these catalyst systems consist of cobalt and a second metal on an oxidic support. In some cases cobalt is the main component, and in others cobalt is an additive increasing the activity of the other metal.

Multi-component systems are often not fully understood. One example is the cobalt-molybdenum system used in hydrodesulfurization. The classical catalyst for this reaction is molybdenum on alumina. Addition of cobalt enhances the activity of the catalyst. This can be explained by several models: The synergism model, the pseudo intercalation model and others /14,103/. But cobalt itself can also have high HDS activity, and the high activity cobalt-molybdenum catalysts have also been attributed to cobalt atoms /3/. Molybdenum may in this case be the "promoter", e.g. by dispersing the active Co phase on the support.

In reactions with synthesis gas hydrocarbons are the main products from cobalt catalysts. Different additives e.g. strontium can, however, increase the selectivity to oxygenates /50/. Other additives enhance the overall activity of the catalysts.

Numerous catalyst characterization investigations of various cobalt catalyst systems have been reported during the last 10 - 15 years /3,6-21/. Independent of the actual application of the catalysts, comparison of the results and conclusions from the different studies will lead to a better understanding of the nature of the supported cobalt catalysts.

2.4 Characteristics of the Co/Al_2O_3 system

The catalysts used in this work were cobalt supported on γ-alumina, and supported cobalt promoted by a noble metal. The catalysts were prepared by impregnation. This was the background for the choice of catalyst characterization literature studied. A summary of the characterization literature is given in Table 2-2 at the end of this chapter.

The structure and valence state of cobalt and the surface composition of the catalyst vary depending on pretreatment and other factors as metal precursors, the kind of support and different second metals added. It is known /10/ that cobalt on alumina surfaces can exist as pure cobalt oxide crystallites of different sizes and also as a mixed spinel with alumina. Islands of cobalt oxides on the support may be expected to reduce in a similar manner as the unsupported cobalt oxide /56/.

Temperature programmed reduction (TPR) has appeared as a proper method for studying metal-support interactions /56.69/. The difference in reducibility is a way to distinguish between different metal oxide phases present on the surface. The method also makes it possible to quantify the amounts of the various phases. For qualitative identification of the oxide-phases it is necessary to use bulk phases of known compounds. Combination with other techniques is also useful and recommended. X-ray Photoelectron Spectroscopy (XPS) and X-ray Diffraction (XRD) are two techniques commonly used together with TPR. TPR spectra of some reference materials are shown in Figure 2-4 /3/.

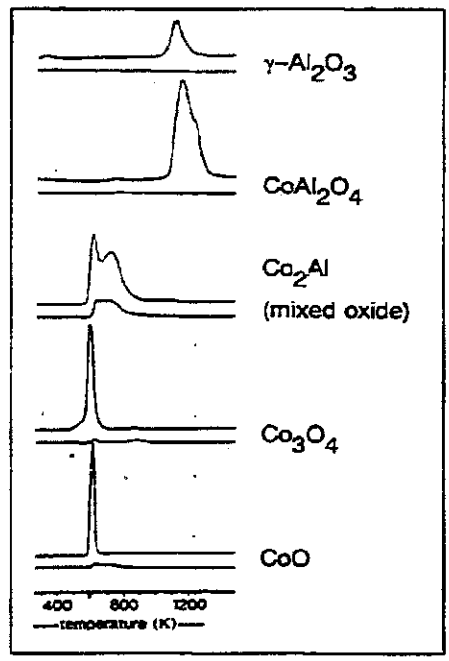

Figure 2-4. TPR patterns of reference materials. From Arnoldy /3/.

2.4.1 Cobalt spinels

The spinel structure is named after the mineral spinel $MgAl_2O_4$ /2/. This structure consists of a cubic closepacked array of oxide ions with Mg^{2+} in tetrahedral holes and Al^{3+} in octahedral holes. Only one eighth of the tetrahedral holes are occupied, and one-half of the octahedral. There are many compounds with the spinel structure, and $CoAl_2O_4$ is one in which the dipositive ions (Co^{2+}) reside in the tetrahedral holes and the tripositive ions (Al^{3+}) in the octahedral. Such compounds are referred to as normal spinels. Co_3O_4 is another example of a normal spinel /3,7/. It can be written $Co(II)Co(III)_2O_4$, corresponding to the relative amounts of Co^{2+} and Co^{3+}.

The $CoAl_2O_4$-spinel is heavily reducible. With TPR it is shown /3,6/ that temperatures higher than 1150 K are required to reduce it. The XPS binding energy for Co^{2+} in $CoAl_2O_4$ is found to be 781.8 ± 0.4 eV /7,8,14/.

TPR peaks for Co_3O_4 are usually found between 550 and 700 K, dependent on apparatus conditions. The TPR behavior of bulk Co_3O_4 is somewhat inconsistent in the literature. Some authors /9,10/ report two separate peaks, while others /3,6,11,12/ observe just one broad peak. When a single peak is observed it appears at almost the same temperature as the narrower CoO-peak. However, whether one or two TPR peaks are observed during the reduction of Co_3O_4, it is generally agreed that Co_3O_4 is reduced in two steps, via CoO:

$$Co_3O_4 + H_2 \rightarrow 3\ CoO + H_2O \qquad (2\text{-}20)$$

$$3\ CoO + 3\ H_2 \rightarrow 3\ Co + 3\ H_2O \qquad (2\text{-}21)$$

This is proved by combination of results from several techniques. When just a single TPR-peak is seen, it is explained /3/ with simultaneous reactions and overlapping peaks.

The characteristic $2p_{3/2}$ XPS binding energy for Co^{2+} and Co^{3+} in Co_3O_4 is 780.3 and 779.5 eV, respectively. It can be difficult to distinguish between these two, but the former is accompanied by a shake up satellite at ~786 eV /9/.

More recent literature /3,11,12/ shows that intermediate phases between Co_3O_4 and $CoAl_2O_4$ are also present on Co/Al_2O_3 catalyst surfaces. In the next sections it will be shown how the distribution of the phases and their reduction behavior, are dependent of cobalt loading, pretreatment conditions, cobalt precursor and promotion with noble metals.

2.4.2 Effect of cobalt loading.

Chin and Hercules /7/ have studied the interaction between metal ions and support in Co/Al_2O_3 catalysts. They studied a series of catalysts with cobalt content varying from 1% to 30%. Their conclusions are based upon studies done with XPS, ISS and SIMS. As the metal concentration was increased there was a consistent decrease in Co^{2+} binding energy in XPS. The catalysts with low cobalt concentration (1 and 2 wt% Co) had binding energies very close to $CoAl_2O_4$, whereas the catalyst of highest metal loading showed binding energies identical with Co_3O_4.

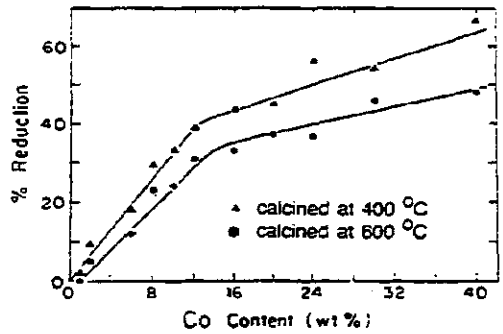

Figure 2-5. **% reduction (from XRD) of Co $/Al_2O_3$ vs. metal loading. Reduced in H_2 for 4 h at 400°C. From /7/.**

An alteration in surface composition as shown in Figure 2-5 did take place at about 10% cobalt. XPS studies of reduced catalysts show that increasing the metal loading up to ca. 12% cobalt causes a linear increase in catalyst reducibility. At this point a break in the curve occurs and the slope becomes lower.

Chin and Hercules found that the metal support interactions lead to tetrahedrally and/or octahedrally coordinated cobalt ions, and they assumed that at low metal concentrations (<10 wt% Co) the cobalt is predominantly in tetrahedral lattice sites of support. At higher cobalt

concentrations an octahedrally coordinated interaction species is produced - and eventually a "bulk-like" Co_3O_4 phase segregates on the surface of the catalyst.

Chung and Massoth /14/ achieved similar results when examining 1 - 4 wt% Co/Al_2O_3 catalysts by thermogravimetry, diffuse reflectance spectroscopy (DRS), XRD and XPS. The catalysts were reduced at 773 K. Below a certain cobalt level (1 - 2 wt% Co) no reduction was observed, whereas above this level the extent of reduction increased with cobalt content. Reflectance spectra showed only tetrahedral cobalt at low cobalt levels, but octahedral cobalt started to appear as the cobalt level increased.

Chung and Massoth support a suggested occurrence of nonreducible and reducible states of cobalt, the former being associated with tetrahedral cobalt, probably located in the Al_2O_3 lattice, and the latter with bulk Co_3O_4. Also changes in colors of the calcined catalysts agree with the above: It turns from light blue via blue-grey to black with increasing amount of cobalt. This is consistent with the colors of $CoAl_2O_4$ (blue) and Co_3O_4 (black) /14/.

TPR-investigations /6,11/ confirm that at low cobalt loadings there is just one, heavily reducible phase, and its reduction temperature fits that of $CoAl_2O_4$. Neubauer /15/ suggests that since the cobalt/alumina-catalysts strongly resist oxidation via exposure to air after reduction, Co^{2+} ions may have migrated into the support during reduction. Tung et al. /11/ showed the existence of a third phase of cobalt oxide, consisting of Co^{2+} and Co^{3+} ions. This is probably an amorphous cobalt oxide overlayer, and its reducibility is between bulk Co_3O_4 and $CoAl_2O_4$-spinel. This phase is observed when the cobalt content exceeds 1%, and is probably deposited over the $ColAl_2O_4$ spinel structure because the DRS-signal from the $CoAl_2O_4$ structure disappears when the cobalt loading increases. The TPR-spectra show two diffuse peaks in the temperature range 600 K - 900 K, and the easiest reducible of these is, from comparison with EPR, suggested to be the reduction of Co^{3+} -species to metal. Tung et al. /11/ state that they cannot observe "bulk" Co_3O_4 in TPR-spectra below 8% cobalt-content. However, this is in disagreement with other work /3/ showing the appearance of "bulk" Co_3O_4 simultaneously with the amorphous overlayer.

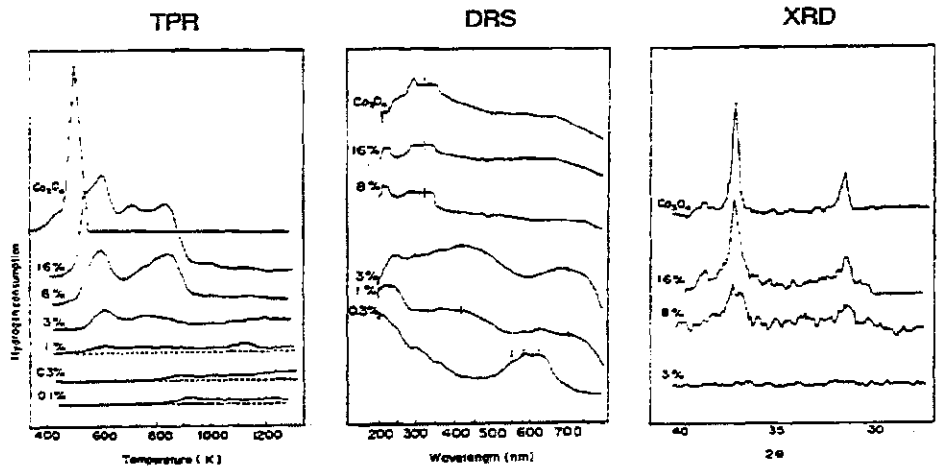

Figure 2-6. TPR, DRS and XRD spectra of cobalt/alumina catalysts with cobalt loading from 0.1 to 16 %. Calcination temperature 773 K. From /11/.

Wang and Chen /6/ also observe a cobalt phase that behaves differently from bulk Co_3O_4 in catalysts with more than 6% cobalt. They point out three different causes:

(I) The smaller particle size for Co_3O_4 on a support makes them more difficult to reduce compared to unsupported Co_3O_4.

(II) Cobalt oxide - cobalt aluminate interactions causing increased difficulty of cobalt oxide reduction.

(III) A species different from Co_3O_4 is present, which is described as a surface Co^{3+} phase.

The relative proportion of the peak at ca. 750 K increases as the cobalt loading increases from 1.5 to 30 wt% Co. The high temperature (>1100 K) peak assumed to be an amorphous surface cobalt-aluminate, shifts to lower temperature with increasing cobalt loading. Wang and Chen /7/ suggest that for high metal loading catalysts, the presence of easy reducible cobalt species may serve as metallic nuclei to facilitate the reduction of other cobalt oxide species which originally interact strongly with the support.

Thus, from studies /3,6,7,11,14,15/ with several techniques the following can be suggested: For catalysts with calcination temperatures in the range 400 - 800 K, about 1% of the cobalt

migrates into the first alumina layers and forms a stable $CoAl_2O_4$ phase which is very difficult to reduce. When the alumina is saturated the surplus cobalt is deposited on the surface as a well spread phase of about a monolayer thickness that interacts with the cobalt aluminate or the alumina, and as small "bulk" Co_3O_4 crystallites. The monolayer containing both Co^{2+} and Co^{3+} ions is growing until the cobalt loading reaches about 10 wt%. Further addition of cobalt gives further formation of, and further growth in the size of the Co_3O_4 crystallites.

2.4.3 Effect of calcination temperature

Arnoldy and Moulijn /3/ investigated a 9.1 % Co/Al_2O_3 catalyst calcined at different temperatures (575 - 1290 K) with TPR, DRS and XRD. They found large differences in reduction behavior depending on the calcination temperature. There was a marked change around 850 K where the solid state diffusion of Co^{2+} ions starts to take place at a reasonable rate. The authors distinguish between four main phases, (I - IV, with subgroups), with TPR peaks around 600, 750, 900 and 1150 K, respectively. A scheme of the various Co phases proposed by Arnoldy and Moulijn is shown in Figure 2-7.

Phase I is Co_3O_4 crystallites, and none of the catalysts examined contained more than 25 wt% of the cobalt as this phase. Phase I disappears at calcination temperatures above 875 K, and it is proposed that the Co^{2+} ions then migrate into the uppermost layers of the alumina structure.

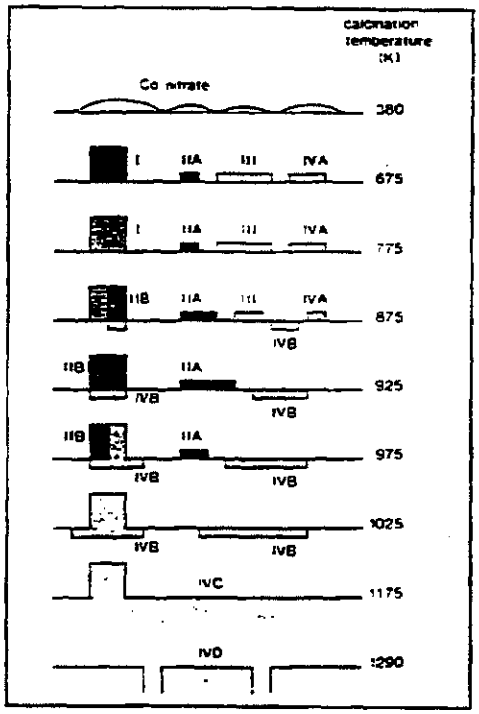

Figure 2-7. Scheme of the various Co phases present on 9.1% CoO/Al_2O_3 as a function of calcination temperature. From Arnoldy and Moulijn /3/.

Catalysts calcined below 825 K contain a dispersed surface Co^{3+} phase, which is called phase IIA. Reduction peaks around 750 K are typical for these Co^{3+} ions.

Arnoldy and Moulijn /3/ suggest that a new phase appear at calcination temperatures above 875 K. Simultaneously as Co^{2+} ions migrate into the alumina structure, Al^{3+} ions from the support replace these ions, resulting in formation of a Co^{3+}-Al^{3+}-oxidic crystalline phase. This phase is called phase IIB. According to energetic reasons Co^{3+} probably occupies the octahedral spinel sites, and Al^{3+} occupy the tetrahedral sites.

Phase III is only observed for catalysts calcined below 950 K. The reduction peak appears at 900 K. This phase is absent in TPR-spectra of the reference materials shown in Figure 2-4. No spinel lines linked with the reduction peak at 900 K are found in XRD. From this it is concluded that it is a non-crystallinic phase interacting with the support, most probably well-dispersed Co^{2+} ions.

Phase IV is assumed to consists of surface Co^{2+} ions with a number of O-Al ligands, which makes them behave chemically like $CoAl_2O_4$. The reduction temperature of phase IV increases with the calcination temperature, and this probably indicates that the lattice stabilization of Co^{2+} ions increases with advancing solid-state diffusion. Catalysts calcined at high temperatures (above 1290 K) consist of stoichiometric $CoAl_2O_4$.

Other investigations with similar /7,8,16/ and other techniques support these findings and conclusions.

2.4.4 Effect of cobalt precursor

For impregnated catalysts, the effects of cobalt starting material on the cobalt-alumina interaction modes and on the dispersion of the resulting cobalt species have received little attention. However, two /8,17/ investigations focusing on the differences in catalyst properties when using nitrate- or acetate-salts as the cobalt precursor have been published recently. Okamoto et al. /8/ found crystalline Co_3O_4 in all the catalysts in the range 5 - 20 % CoO on Al_2O_3 from XRD-analysis when using cobalt nitrate as the starting material and 673 K as

calcination temperature. In catalysts prepared from cobalt acetate and with the same cobalt loading and calcination temperature, no XRD-peaks due to Co_3O_4 appeared. From this they suggest more extensive interaction of cobalt with Al_2O_3 for Co/Al_2O_3(acetate) than for Co/Al_2O_3(nitrate). Their TPR results confirm these assumptions, and show that for Co/Al_2O_3(acetate) a cobalt-aluminate compound is dominant, while only a weak Co_3O_4-peak is observed. When the catalyst is calcined at 823 K this small Co_3O_4-peak disappears. Co/Al_2O_3(nitrate) gives a quite different TPR-spectrum, resembling the results reported by Arnoldy and Moulijn /3/ for a similar catalyst. Co_3O_4 and surface cobalt phases containing Co^{3+} ions are shown to be present in the Co/Al_2O_3(nitrate) catalyst. The total H_2 consumption for the catalysts from acetate were lower than for the catalysts from nitrate. Using these results in combination with XPS-data Okamoto et al. conclude that the cobalt species in Co/Al_2O_3(acetate) are more dispersed than in Co/Al_2O_3(nitrate), although the total amount of surface cobalt are lower due to extensive reactions of Co^{2+} with Al_2O_3. The presence of Co_3O_4 and the lower cobalt dispersion for the nitrate catalysts are proposed to result from oxidation of Co^{2+} in the cobalt nitrate to Co^{3+} during the calcination by nitrate anions. Roynek and Polansky /17,18/ agree with this conclusion and suggest that the Co^{3+} ions do not interact strongly with the alumina, and therefore agglomerate on the surface to Co_3O_4.

2.4.5 Promotion with noble metals

It is generally /23/ agreed that addition of a second, noble metal facilitates the reduction of the first, non-noble metal, but there is still much uncertainty about the mechanisms of the reduction promotion effect and the effect on activity and selectivity of the catalysts. Is the noble metal more than a reduction promoter?

Characterization of bimetallic systems is considerably more difficult than characterization of monometallic systems. The metals may form other surface structures due to the interactions between the two metals and the support. Several probabilities have to be considered, such as /47/:

- Different particles may have different metal content.
- The miscibility of the components may be a function of particle size.

- The particles may have concentration gradients between the surface and the center of the particle.
- The particle size and composition can be affected by the support.
- The particle "characteristics" may also alter as a function of pretreatment, temperature and reactive environment.
- Changes in oxidation states for one or both components can occur during the reaction.

Investigations of different catalyst systems reported in the literature are referred below. They clearly show the complexity of the bimetallic systems.

Sass et al. /19/ investigated Co/Al_2O_3 and $Co\text{-}Pd/Al_2O_3$ (0.8-3.0 wt% Co. 0.05-0.5 wt% Pd) catalysts by ESR and DRS. They found that palladium addition to cobalt-alumina catalysts results in easier reduction (after oxidation at 773 K. 200 mm Hg. 1 h) of Co^{2+} ions to the metallic state. Only the absorption bands of octahedral Co^{2+} (20 % of Co^{2+} in $CoAl_2O_4$ are proposed to have octahedral coordination) and Co_3O_4 vanish in a hydrogen atmosphere (T=873 K. 200 mm Hg. 1 h) for Co/Al_2O_3. while for $Co\text{-}Pd/Al_2O_3$ these changes is accompanied by a significant decrease in the intensity of the absorption bands for tetrahedral Co^{2+} (in $CoAl_2O_4$). These effects appear even at small concentrations of palladium. and are believed to be due to a palladium-promoted formation of a finely dispersed metallic cobalt phase. They also found that for prereduced. reoxidized catalysts the amount of octahedral Co^{2+} decrease with increasing palladium content. The amount of Co^{3+} is significantly greater in the cobalt-palladium catalysts compared to the cobalt catalysts. This shows that palladium promotes the oxidation of Co^{2+} to Co^{3+}. Oxidized. not prereduced catalysts do not show a difference in the Co^{3+}-content. confirming that the Co^{2+} originates from the dispersed metallic cobalt. and not from the tetrahedral Co^{2+} in the $CoAl_2O_4$ spinel.

Belousov et al. /20/ studied the reduction behavior at low temperature (77-300 K) and under low pressure (0.01-0.07 kPa) on unsupported Co_3O_4 and on Co_3O_4 doped with 0.5 wt% PdO. XPS showed that for Co_3O_4 the vast majority of Co(III) surface atoms are not transferred to the Co(II) state. while for the $PdO\text{:}Co_3O_4$ system hydrogen reduces all Co(III) to Co(II) and also a small amount of Co(0) has been observed. The authors believe palladium plays an

active role in the reduction mechanism in the transfer of oxygen from the oxide bulk through the palladium aggregates to vacuum.

Guczi et al. /21,22/ studied a series of $Pt_{1-x}Co_x/Al_2O_3$ bimetallic catalysts with 10% total metal loading with XPS and TPR. The atomic fraction of Co, varied from 0 to 1.0. The catalyst pretreatment was mild; with calcination and reduction at 570 K for 1 h. XPS of the reduced cobalt-platinum catalysts showed two peaks: The first indicated cobalt metal (778,1 eV). The second was attributed to an unreduced cobalt surface phase (782,0 eV), interpreted as a surface spinel or a mixed oxide phase with Co^{3+} and Co^{2+} in octahedral lattice sites in close contact with the support surface. The XPS-spectrum for the cobalt catalyst (X = 1.0) did not show any cobalt metal peaks. A peak appearing at 780,5 eV was assigned to CoO, and proposed to be the result of the first step in Co_3O_4 reduction. The absence of the 780,5 eV peak for the platinum containing catalysts was explained by a complete reduction of the CoO phase to Co metal in the presence of platinum.

The amount of platinum on the surface remained constant with increasing cobalt content, while the cobalt amount on the surface is increasing. This means that the surface is enriched in cobalt for the catalysts with high cobalt loadings, but also that the dispersion of metallic platinum increased with decreasing platinum loading. The dispersions calculated from XPS are high and constant for ionic cobalt (the surface phase) in the cobalt-platinum catalysts. For metallic cobalt there is a weak decrease in dispersion with increasing cobalt loading. This is in agreement with the common trend referred to in chapter 2.4.2. The cobalt catalysts (X=1) showed low ionic dispersion, and this is explained with the presence of a cobalt oxide phase with low dispersion, CoO.

As expected from the XPS results, investigation of the same catalysts by TPR /22/ gave a shift to lower reduction temperatures of the cobalt when platinum was present. In contrast to Belousov et al./20/, Guczi et al. explain this effect with the high dispersion of platinum giving a large interface with the cobalt oxide. Hydrogen atoms generated on reduced platinum sites facilitate the reduction of cobalt oxide. They assume that with high cobalt loading, large cobalt oxide particles exist associated with small platinum particles. During reduction partly bimetallic particles are formed. Formation of Pt_3Co and PtCo was found by EXAFS and XRD

after reduction of $Pt_{0.6}Co_{0.4}$ on alumina /133/.

Alloy formation to some extent is also proposed by Dees and Ponec /48/. They suggest that the metal surface is enriched in cobalt. If no segregation of the alloy takes place, a second unalloyed cobalt phase or a cobalt-rich alloy is also expected to be present. Similar metal phases are found for cobalt-iridium on alumina catalysts /49/.

Niemantsverdriet et al. /23/ investigated bimetallic catalysts of 5 wt% Fe, Ni or Co and noble group 8 metal in a 1:1 atomic ratio on silica and concluded that the metals were intimately mixed. All these catalysts were reduced at lower temperatures than needed for the non-noble monometallic catalysts and it is suggested that the reduction of the non-noble metal is catalyzed by the noble metal. Mössbauer spectra showed that reduced iron forms an alloy with the noble metal, and therefore spillover and long distance migration of H atoms over the support were not necessary.

It is also shown /12/ that rhodium facilitate the initiation of the reduction of cobalt via dissociative adsorption of hydrogen on reduced rhodium. van't Blik and Prins /12/ discuss several possible mechanisms:

(I) The two metals precursors are in close contact.
(II) The reduced rhodium metal atoms are able to diffuse over the support surface and aid in the reduction of the metal ions they encounter.
(III) Hydrogen atoms spillover from metallic rhodium particles via the support to the cobalt ions.

Alternative (III) is rejected because their TPR results /12/ indicate that metallic rhodium and cobalt particles are not separately present after reduction. It is earlier reported that cobalt and rhodium are completely miscible /25/. Together with own XRD and TPR investigations of unsupported Co-Rh mixtures, van't Blik and Prins takes this as support when they suggest that bimetallic particles are most probable. Furthermore, through EXAFS studies of reduced $Co\text{-}Rh/SiO_2$ van't Blik et al. /26/ show that rhodium atoms have rhodium as well as cobalt neighboring atoms.

Hydrogen chemisorption results /12/ show that the dispersion of the bimetallic catalysts and monometallic cobalt catalysts is significantly lower than the dispersion of the monometallic rhodium catalyst. It is assumed that cobalt on the monometallic catalyst was poorly dispersed on alumina before reduction. A suggested explanation of this is sintering of cobalt oxide, formed by decomposition of $Co(NO_3)_2$ during drying. The lower dispersion of the bimetallic catalysts can be caused by the presence of cobalt nitrate or cobalt surface spinel that hinders the formation of a well dispersed $RhCl_3$ phase on the alumina surface during the impregnation and drying step /12/.

When TPR-spectra /12/ of bimetallic catalysts are compared to TPR-spectra of monometallic cobalt catalysts, a shift to lower temperatures is seen for the cobalt reduction peak. This shift to lower temperature is not seen for reduced, reoxidized bimetallic catalysts. From this alloy formation is assumed to take place during reduction. The surface of the reduced bimetallic particles is suggested to be enriched in cobalt, while the core is enriched in rhodium. When rhodium is covered by a cobalt rich layer it is not able to facilitate the reduction of the cobalt oxide any more. Thermodynamics predict that cobalt having the lowest sublimation energy will be preferred in the surface region of the alloy /27/. This tendency will be strengthened when the catalyst is exposed to oxygen at room temperature, because the interaction between oxygen and cobalt is stronger than the interaction between oxygen and rhodium ("gas-induced surface enrichment" /135/). Figure 2-8 illustrates the changes in structure of the Co-Rh particles after different treatments suggested by van't Blik and Prins.

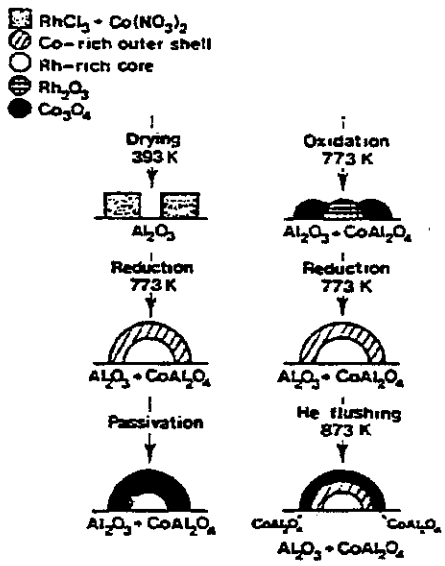

Figure 2-8. Formation of bimetallic CoRh particles during different treatments. From van't Blik and Prins /12/.

Both cobalt and ruthenium are active catalysts in Fischer-Tropsch synthesis. In alumina supported cobalt catalysts doped with ruthenium Shpiro et al. /29/ found bimetallic Ru-Co particles of fairly uniform composition, but also nonreduced cobalt oxide and surface aluminate. Mixed clusters of $RuCo^+$ were found in mass spectra, and combined with XRD results, they were taken as evidence for alloy formation. These catalysts had higher extent of reduction than the monometallic catalysts. The authors explain this by the activation of H_2 on ruthenium and its spillover to cobalt oxide, as well as alloy formation and weakening of the interaction of ruthenium with the alumina.

Table 2-2. A summary of the Co catalyst characterization literature in Chapter 2-4.

Catalytic system	Application	Investigation techniques	Investigated parameters	Ref
Co/SiO_2	FT[b]	TPR, XPS, at[a]	Co precursors	Polansky/17,18/
Co/Al_2O_3	FT[b]	TPR, XRD, at[a]	Co loading, activity	Wang /6/
Co/Al_2O_3		TPR,DRS,XRD,EPR	Co loading	Tung /11/
Co/SiO_2	FT [b]	TPR, XPS	Oxidic promoters	Sexton /9/
Co/Al_2O_3	HDS[c]	TPR, XRD, DRS	Calc.temp.	Arnoldy /3/
Co/Al_2O_3	HDS[c]	XPS, ISS, SIMS	Co loading, Calc.temp.	Chin /7/
$Co(Mo)/Al_2O_3$	HDS[c]	SEM, XPS, DRS.	Preparation, Calc.temp	Chung /14/
Co/Al_2O_3	HDS[c]	TPR, XPS, XRD	Co precursors	Okamoto /8/
Co/Al_2O_3	HDS[c]	TPR, XPS	ZnO addition	Okamoto /16/
$CoRh/Al_2O_3$		TPR, TPO	Co - Rh	van't Blik /12/
Co/Al_2O_3		TPD,Moessbauer,at[a]	Co - support	Neubauer /15/
$Co,Fe,Ni/Al_2O_3$	Ammonia synt.	TPR	Fe-Co, Fe-Ni	Brown /10/
	Lit.review	TPR		Hurst /56/
$CoPd/Al_2O_3$	Oxidation rx.	ESR, DRS,	Co and Pd loading	Sass /19/
Pd/Co_3O_4		XPS,	Co-Pd, reduction	Belousov /20/
$PtCo/Al_2O_3$	Methanol activation	XPS, H_2/CO Chem., TPR, D exchange	Pt-Co loading,	Guczi /21,22/
$PtCo/Al_2O_3$	Reforming	XRD, at[a]	Pt-Co loading	Dees /48/
$CoIr/Al_2O_3$	FT[b]	TPR, at[a]	Co-Ir loading	Guczi /49/
$CoRu/Al_2O_3$	FT[b]	XPS, UV, at[a]	Co-Ru loading	Shpiro /29/

[a] at = activity tests
[b] FT = Fischer Tropsch reaction
[c] HDS = hydrodesulfurization

2.5 Activity and selectivity

In this chapter it will be seen how the activity and selectivity are affected by the degree of reduction, the dispersion and crystallite size, and the cobalt loading. These factors will be discussed in view of the results referred to in the former chapter. Mono-metallic systems as well as bimetallic, will be treated.

2.5.1 Reduction extent and dispersion

Cobalt/alumina systems have been studied for several years /30-39/. The relations between hydrogen and carbon monoxide adsorption and the degree of reduction is of great interest when discussing variations in activity and selectivity.

Dispersion is defined as the ratio of surface metal atoms to the total amount of metal atoms. The number of surface atoms may be determined from chemisorption of hydrogen or carbon monoxide. However, Bartholomew /35/ assumed that the chemisorption just takes place on reduced metallic sites, and modified the dispersion definition, taking account for this:

$$D = \frac{N_s}{N_{tot} \cdot f} \qquad (2\text{-}22)$$

where N_s - number of surface atoms, measured by H_2 chemisorption
N_{tot} - total number of metal atoms
f - fraction of cobalt reduced to metal, determined from O_2 titration

This way to calculate the dispersion is widely used, also in the literature referred to later in this chapter. If not otherwise noted, Bartholomew's definition is used. A common method for determination of the extent of reduction to cobalt metal is volumetric O_2-titration of reduced samples at 673 K, assuming stoichiometric formation of Co_3O_4 /35/.

By use of O_2 titration and H_2 chemisorption Bartholomew and others /30,33,35,38/ found that the cobalt particle size and the degree of reduction increased with increasing cobalt loadings.

The dispersion of the reduced metal decreased with increasing cobalt loading. These trends are in agreement with the formation of different cobalt oxide phases as discussed in Chapter 2.4.2: With high (25 %) cobalt loading a large fraction of the cobalt exists on the support surface as easily reducible Co_3O_4, while with 3 % cobalt loading, most of the cobalt is present as heavily reducible cobalt aluminate spinel /7,14/. However, from this it is difficult to say whether the decrease in dispersion is an effect of reduction extent or of particle size.

When Lee et al. /38/ kept the metal loading constant they could not, by use of TEM, observe any changes in the crystallite size with increasing reduction extent, when reducing at mild conditions (temperatures below ca. 700 K). The reduced metal dispersion increases with increasing reduction extent when the time and temperature are increased, while the $CO:H_2$ adsorption ratio decreases with increasing reduction extent /38/. Moon and Yoon /36/ could also observe increasing degree of reduced metal dispersion with increasing degree of reduction, when increasing the reduction extent by increasing the reduction time at 648 K.

With an increase in the reduction temperature above 700 K the dispersion decreases /33,36/ or stabilizes /38/ with increasing reduction extent. This occurs simultaneously with a decrease and subsequent stabilization in the $CO:H_2$ adsorption ratio.

It is suggested /36,38/ that large amounts of unreduced cobalt oxide at low degrees of reduction modify the electronic properties of the reduced cobalt metal. This could cause a suppression of H_2 adsorption. A consequence of this is that the dispersion will be underestimated at low extent of reduction when it is calculated from hydrogen uptake.

In the high reduction temperature case, Moon and Yoon /36/ suggest formation of stable cobalt - alumina compounds as the cause of decreased dispersion with increasing reduction extent. At high reduction temperatures decoration is suggested by Huang et al. /40/ to occur on Ni/Al_2O_3, and result in a decreased dispersion. The decoration phenomenon was explained by the appearance of Al_xO_y-aggregates on the metal surface, formed from thermally promoted diffusion of Al^{3+} ions from the $NiAl_2O_4$. Decoration would lead to lower H_2 adsorption, while the stronger CO adsorption would not be affected.

2.5.2 CO hydrogenation activity

The CO hydrogenation activity of a catalyst can be measured as the CO conversion per gram of catalyst (or gram of active metal) per second. However, often just a small part of the metal present on the catalyst is exposed to the surface, this will vary with e.g. metal particle size. The specific activity or turnover frequencies (TOF) are therefore more convenient than global activity comparisons for systems with a broad particle size distribution and non-uniform composition. TOF is defined as the number of CO molecules converted per catalytic site per second /31.43/. A standard measure of the number of active sites on the metal surface is chemisorption of CO or H_2 (the dispersion). As discussed in the previous chapter the dispersion is dependent on several factors, and thus the TOF will as well vary with e.g. reduction conditions and metal loading.

Turnover frequency, increases with increasing cobalt loading /30.38/, when the reduction conditions are kept constant. Results from Fu and Bartholomew /33/ are shown in Figure 2-9. At that time, Bartholomew explained the variations in TOF with increasing metal loading with:

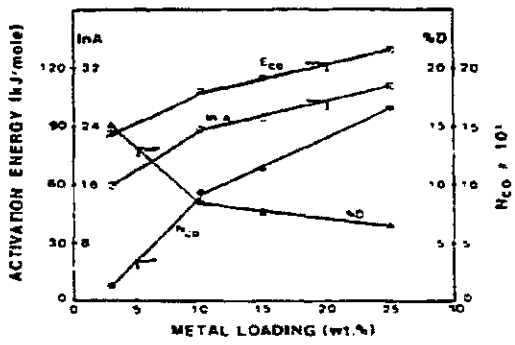

Figure 2-9. Dispersion, TOF, E_{CO} and ln A for CO hydrogenation on Co/Al_2O_3 catalysts of different loading. From /33/.

- Increase in the relative concentration of surface sites with low coordination numbers due to decreasing dispersion.
- Changes in electronic structure induced by increasing degree of interaction between support and metal with decreasing particle size.
- Changes in binding energy for intermediate products due to changes in surface structure when particle size vary.

These arguments led to the conclusion that the reaction is structure sensitive. However, more recent investigations have shown that some of these changes may be due to variation in the extent of reduction rather than the particle size.

Lee et al. /38/ found (when keeping the metal loading constant, and varying the degree of reduction by increasing the reduction temperature) that the specific activity for CO hydrogenation passed through a maximum between 10 and 20 % reduction. From Figure 2-10 /38/ it is seen that this is valid for different cobalt loadings. The TOF starts to decrease at about the same reduction level at which the reduced metal dispersion and the $CO:H_2$ adsorption ratio stabilize.

Moon and Yoon /36/ found increasing TOF for methanation with increasing extent of reduction: When the reduction temperature was kept constant at 648 K, and the reduction time was increased, a reduction extent around 20 % gave 5 - 10 times higher methanation activity compared to reduction extent above 30%. However, both in this /36/ and other studies /33/ both the total TOF and the TOF for methanation pass through a local maximum when reduction extent increases as a result of increasing the temperature above 700 K. The dispersion is somewhat lower, and the specific activity somewhat higher for the same reduction extent when it is achieved at high temperatures rather than long time at low temperature.

Palmer and Vroom /39/ have shown significantly higher activities on partially reduced cobalt and nickel foils, compared to clean metal surfaces.

The activation energies for both methanation and CO conversion are increasing with increasing degree of reduction, independent of the dispersion level /36,30/. In recent

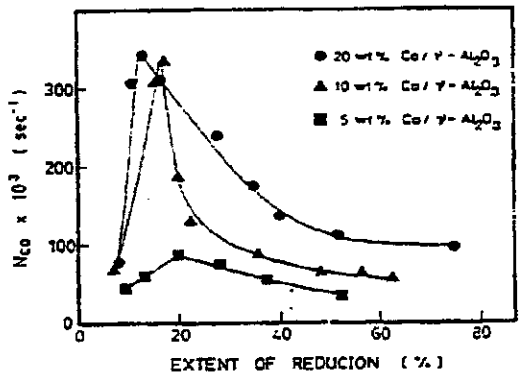

Figure 2-10. Changes in TOF (from H_2 ads.) with reduction extent. Reaction at 1 atm., 250°C, $H_2/CO=3$. From /38/.

investigations of well dispersed iron on alumina catalysts. Rameswaran and Bartholomew /42/ show that when the reduction extent is kept constant (in the range 30 - 50 %), the activity is independent of dispersion. Similar observations are made for cobalt, as well as nickel catalysts /43,144/. These results indicate that CO hydrogenation is a structure insensitive reaction on Fe, Co and Ni. This is also supported by studies /44/ of CO hydrogenation on cobalt deposited on W(110) and W(100). These results suggest that initial geometry does not play a significant role in determining the steady-state activity on cobalt surfaces.

The remaining question is therefore: What are the reasons for the apparent variation in activity with varying degree of reduction?

The phenomenon in Figure 2-10 was explained by Lee et al. /38/ with the presence of electronic interaction between the oxidic cobalt surface phase and the metal phase of cobalt, which is suggested to enhance the CO hydrogenation activity and suppress the H_2 adsorption. Both factors give increased apparent TOF. The size of the interface between the two phases will vary depending on the degree of reduction, and a maximum in interface area is expected.

The lower dispersion and higher activity at a given extent of reduction for catalysts reduced at increasing temperatures, may be due to the decoration effect, as suggested by Rameswaran and Bartholomew /42/. The suppressed H_2 adsorption that results from this, will give an apparent increase in TOF when the TOF calculation is based on H_2 chemisorption.

2.5.3 CO hydrogenation selectivity

Increasing the cobalt loading of the catalysts (and thereby also increasing the degree of reduction) was found to give less CO_2 formation and longer hydrocarbon chains /30,38/. Both the C_1 and the C_2 selectivities decrease, while the C_{5+} fraction increases with increasing cobalt content. Simultaneously the olefin/paraffin ratio decreases /33,38/. When the cobalt content is kept constant, such a marked change in chain length is not observed when the reduction extent is increased by changing the reduction time. A slight increase in the average chain length with the degree of reduction is observed when the reduction temperature is 773 K (Table 2-3) /38/. The opposite - a slight decrease - is observed when the reduction

Table 2-3. Changes in hydrocarbon product distribution with cobalt loading, reduction time and reduction temperature. From Lee et al. /38/.

Catalyst[a]	Reduction extent (%)	Conversion (%)[b]	Product distribution (wt%)					$\frac{C_{=2}}{C_2}$	$\frac{C_{=3}}{C_3}$
			C_1	C_2	C_3	C_4	C_5		
2-500-10	48.6	1.7	68.1	10.4	11.7	8.9	0.9	0.61	0.74
5-500-10	52.5	1.7	61.4	12.7	16.5	7.4	2.0	0.32	0.44
10-500-10	56.6	1.8	49.6	10.1	18.1	12.4	9.8	0.18	0.31
20-500-10	74.4	1.7	41.1	8.1	20.1	18.4	12.3	0.17	0.31
10-300-0.7	7.9	1.7	50.6	11.0	20.4	12.1	5.9	0.21	0.39
10-300-4	15.4	1.9	50.3	10.6	19.6	11.5	8.0	0.23	0.37
10-350-4	17.2	1.8	52.2	10.5	19.3	11.2	6.8	0.20	0.32
10-400-4	19.5	1.8	51.4	9.5	19.4	11.1	8.6	0.13	0.36
10-450-4	22.5	1.8	49.2	10.6	18.6	11.7	9.9	0.14	0.33
10-500-4	35.7	1.9	51.1	9.6	17.8	12.1	9.4	0.21	0.29
10-500-10	56.6	1.8	49.6	10.1	18.1	12.4	9.8	0.18	0.31
10-500-20	62.8	1.9	48.5	10.5	18.7	12.3	10.0	0.16	0.31
10-525-4	48.6	1.7	50.4	9.8	18.3	11.8	9.7	0.15	0.33

[a] Catalyst notation: Cobalt loading, wt% - reduction temperature, °C - reduction time, h
[b] Reaction conditions: 1 atm, 250°C, $H_2/CO = 3$.

temperature is 648 K /36/.

There are also disagreements between these two studies /36,38/ when comparing changes in olefin/paraffin ratio as a function of the reduction extent. Lee et al. /38/ did not find any effects on the olefin selectivity, while Moon and Yoon /36/ found that the selectivity to unsaturated hydrocarbons increased for the poorly reduced catalysts. In this case the CO conversion was very low and increasing (0.2 - 1.8 %) with increasing degree of reduction. Moon and Yoon /37/ have later shown that the ethylene/ethane ratio decreases with increased degree of reduction at constant CO conversion.

Moon and Yoon /36,37/ explain the increase in olefin/paraffin ratio with increased reduction extent with suppressed H_2 adsorption. H_2 adsorption is assumed to be suppressed at low degrees of reduction /38/, and when decoration with Al_xO_y agglomerates covers parts of the

reduced metal when reduced at high temperatures. Lower H_2 concentration on the surface will reduce the rate of secondary hydrogenation of the primary olefins.

Changes in average carbon number depend on how the propagation and termination rates change relative to each other /38/. Fu and Bartholomew /33/ initially suggested that changes in this ratio is due to changes in the adsorption strength of carbon containing intermediates. TPD-studies done by Reuel and Bartholomew /30/ show a shift from weakly bound carbonyl species to strongly bound CO species with increasing cobalt loading. This would lead to higher residence times, lower termination rates, and therefore longer chains. More recent studies reported by Lee and Bartholomew /45/ indicate that two different (A and B) reaction states or mechanisms for CO hydrogenation are present. The more active A state is attributed to hydrogenation of atomic α-carbon on large three dimensional cobalt crystallites, while the less active B state is assigned to decomposition of a CH_xO complex originally formed on the support from spilled-over hydrogen and carbon monoxide. This can take place on both large and fairly inaccessible small metal crystallites. The fraction of methane formation via reaction A relative to reaction B increases with increasing metal loading and reduction temperature.

Lapidus et al. /46/ suggest that the carbon monoxide methanation centers and those of the hydrocarbon chain growth are different in nature. The sites for the mechanism involving interaction with the support or oxidic metal on the surface, is thought to be responsible for the formation of liquid hydrocarbons.

Changes in the cobalt loading have the strongest effect on selectivity. Lee and Bartholomew /45/ propose that a high density of metal crystallites in the higher loading catalysts gives a shorter path for surface diffusion of the methoxy species (mechanism B referred to above) from the surface to the metal. Lee et al. /38/ suggest that changes in the adsorption strength of carbon-containing intermediates may explain the increased production of higher hydrocarbons with increasing cobalt loading.

Decoration taking place at high reduction temperatures favours CO adsorption relative to H_2 /40/ and this may explain the slight increase in chain growth observed at high reduction temperatures /38/. The slight decrease in chainlength with increased reduction time at low

reduction temperatures, may be due to a increasing H_2 uptake with increasing reduction time /36/. This is supported by a decreasing CO:H_2 adsorption ratio with increasing reduction time found by Lee et al. /38/ in the same range of reduction-temperatures.

2.5.4 Activity and selectivity of bimetallic Co-systems, compared to monometallic systems.

The main reason for using bimetallic catalyst systems is to enhance activity and stability and/or to modify the selectivity. Many kinds of factors may contribute to the overall effect /47/:

- The metallic particles can be altered in size, composition and in electronic structure.
- Modifications in adsorption characteristics and in surface coverage of reactive intermediates can take place, leading to changes in selectivity.
- The reducibility of the "main" metal (e.g. Co) can be improved.

All these factors make it difficult to get a clear picture of the mechanisms involved. The heterogeneity of the metal particles on the catalysts introduces complications when trying to explain the observed changes in activity and/or selectivity following by promotion.

The difficulties in determination of dispersion and turnover frequency for monometallic systems due to e.g. suppression of hydrogen adsorption or CO adsorption on support are small compared to the problems which may appear when investigating bimetallic systems. The adsorption mechanisms are much more complex on bimetallic catalysts /47/, and depend on the properties of both metals. The H_2 adsorption can be either suppressed or increased relative to the real number of active sites. Enhanced H_2 adsorption can be caused by either spillover from metal A to support or to metal B (possibly inactive in H_2 dissociation). Suppression of H_2 adsorption can be caused by blocking surface of metal A with inactive metal B. It is known /47,101/ that H_2 adsorption demands ensembles of several metal surface atoms in a specific configuration. Such ensembles can be disturbed by the addition of a second metal. These complications make it important to know the properties of the two metals that are combined, in order to interpret the chemisorption.

The surface coverage of H_2 relative to CO is an important factor for the resulting activity and selectivity. Changes measured with H_2 and CO chemisorption can therefore give a contribution to the understanding of observed changes in activity and selectivity. But due to the complexity in interpreting the chemisorption data few use turnover frequencies in bimetallic cobalt catalysis. Most of the activity data available for bimetallic cobalt catalysts are therefore expressed as [CO conversion per gram of catalyst (or gram of metal) on alyst].

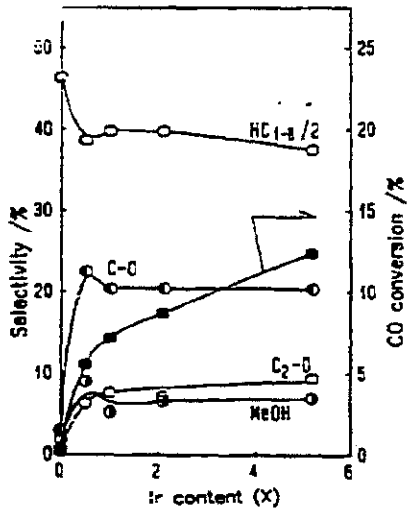

Figure 2-11. Effect of Ir content in silica supported Co-Ir catalysts, derived from Co-acetate. Co:Ir:SiO_2 = 5:X:100 /50/.

Matsuzaki et al. /50,51,52/ studied changes in the activity and selectivity in CO hydrogenation to oxygenates over silica supported cobalt catalysts promoted with iridium, rhenium and ruthenium. They varied the precursor and the loading of the second metal. Even though the pure Re, Ru and Ir show different behavior in CO hydrogenation, they behave similarly as modifiers of catalysts derived from cobalt acetate, by enhancing the CO conversion and the selectivity to oxygenates (Figure 2-11). Ru and Ir on cobalt catalysts derived from $Co_2(CO)_8$ showed little effect on activity /136/. The carbonyl derived catalysts are well dispersed and well reduced even without a promoter. From this the authors /50/ suggest that the main role for the second metal is to be a promoter in reduction of divalent cobalt to the metallic state by hydrogen spillover, and such making more cobalt metal available. The well dispersed cobalt metal is proposed to be the principal active center for CO hydrogenation to oxygenates.

Ir-promoted cobalt on alumina catalysts studied by Guczi et al. /49/, showed different activity and selectivity behavior, depending on the amount of iridium. As seen in Figure 2-12,

addition of small amounts of iridium increases the CO conversion rate. However, further addition results in a sharp decrease in the reaction rate, the activation energy (Figure 2-12) and in the olefin production (Figure 2-13), yielding mainly methane which is the characteristic product from CO hydrogenation on iridium. Chemisorption data shows decreasing H_2 adsorption with increasing cobalt content, and this is probably related to the existence of activated hydrogen chemisorption on cobalt, as found by Bartholomew /53/. Reactive carbon is suggested to be formed from dissociated CO, which easily occurs on metallic cobalt. The CO hydrogenation rate is assumed to be controlled by CO dissociation. Deactivation is also explained to take place due to carbide formation. Weakly bound hydrogen is not assumed to be available on cobalt, due to the chemisorption of activated hydrogen. Chain propagation of reactive carbon

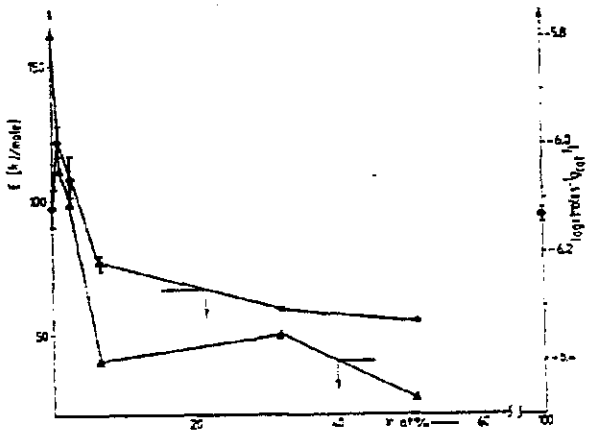

Figure 2-12. Log rate and activation energy vs. composition. Co-Ir/Al_2O_3. From /49/.

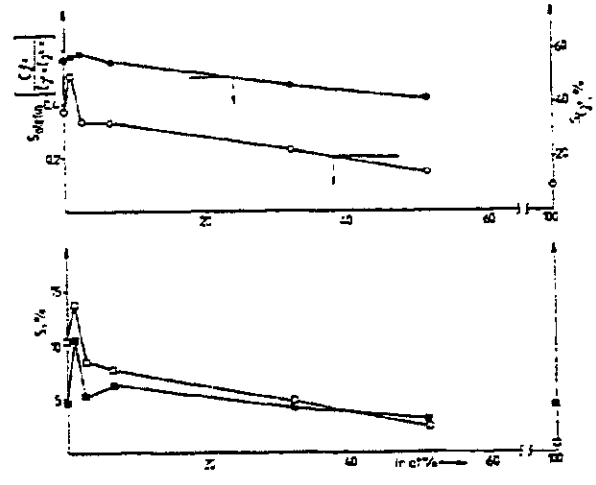

Figure 2-13. Selectivities for a) olefins and hydrocarbons (C_{2+}), and b) ethylene and propylene. From /49/.

is therefore expected to be dominating. This gives long hydrocarbon chains, mainly olefins, as the product. As opposed to Matsuzaki /50/, Guczi /49/ assumed that iridium is directly involved in the changes in activity and selectivity. Small amounts of iridium in the surface cobalt matrix decrease the overall activity, but increased hydrogen supply from iridium prevents deactivation. More reactive carbon will appear on the surface and enhance the chain growth and olefin formation. Further iridium addition will split up cobalt ensembles responsible for CO dissociation and result in decreased chain growth. At the same time the increased iridium content will give weakly bound hydrogen, and higher hydrogenation activity, yielding less olefins and more methane. The decrease in activation energy is supposed to be a result of decreased carbide formation when iridium is added.

In contrast to Matsuzaki /50/, Guczi et al. /49/ do not report formation of oxygenates over cobalt-iridium catalysts. This fact, and also the different trends in CO hydrogenation rate with increasing iridium content, may be due to differences in the support, the cobalt precursor and the pretreatment, as well as reaction conditions. These factors may lead to quite different surfaces for the catalysts, and e.g. the degree of contact between cobalt and iridium may determine the effect of iridium. It can be noted that Matsuzaki et al. /50/ reduced the cobalt catalysts before impregnation with iridium. This could prevent the formation of bimetallic alloys, which were claimed to be present in the catalysts studied by Guczi et al. /49/.

Guczi et al. have also published kinetic investigations of the $Pt_{1-x}Co_x/Al_2O_3$ (x=0-1, Pt+Co=10 wt%) system /22/. As presented in Figure 2-14 the reaction rate shows a behavior much like that of Co-Ir systems /49/. Small amounts of platinum enhance the total

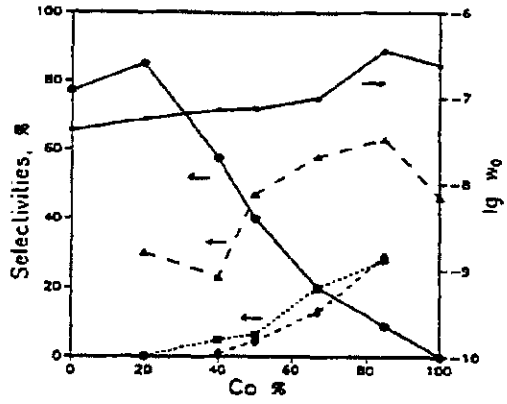

Symbols: (•) log r_o, total reaction rate, log (mol/s g of catalyst); Selectivities: (▲) for C_{2+} hydrocarbons; (■) for olefins; (●) for oxygenates including DME; (▼) for ethanol (in the total oxygenates).

Figure 2-14. Product selectivity and rate of CO/H_2 reaction vs. bulk concentration of Co in $PtCo/Al_2O_3$ catalysts. From /22/.

rate, but further addition of platinum (and decreasing cobalt amount) leads to decreased CO hydrogenation rate. The enhanced rate at low Pt loading is suggested to be due to the existence of platinum with active sites for dissociation of hydrogen. It is also shown that platinum facilitate the reduction of cobalt. The observed increase in ethanol selectivity is explained with the presence of zerovalent cobalt and thus Co sites capable for CO dissociation. The resulting CH_x units are available either for chain growth, or CO insertion which is assumed to require platinum sites.

If platinum had existed as a separate phase, it is expected to be well dispersed when present in small amounts. Since platinum is proposed to be responsible for CO insertion giving oxygenates, the yields of oxygenates is taken as an indicator showing if platinum is present as a separate phase or not. Therefore it was suggested that the decrease in overall oxygenate selectivity with increasing cobalt loading is evidence for formation of bimetallic particles.

Addition of palladium to silica- and alumina-supported 5-10 wt% Co catalysts has been investigated by Lapidus et al. /54/. They found changes in activity and selectivity to some extent similar to those reported by Guczi et al. /22,49/: The introduction of 0.3 - 0.5 % Pd led to an increase in the activity and in the selectivity to liquid hydrocarbons. The yield of C_{5+} products increased by a factor of 1.3. A further increase in the Pd content to 1 - 3 % turned the positive effect to the opposite. Then a decrease in the CO conversion as well as in the yield of liquid hydrocarbons was observed. Shielding of some of the active cobalt centers by palladium on which CO is adsorbed molecularly, was suggested as an explanation of the decrease in activity /54/. Alloy formation or changes in particle size, however, was not discussed as an explanation for the decreased activity.

Iridium, platinum and palladium are all relatively inactive in CO hydrogenation compared to cobalt. Ruthenium, however, is known to give higher TOF and higher selectivities to long chain hydrocarbons than cobalt /29,125/. Shpiro et al. /29/ studied the effect of adding ruthenium to cobalt (2 wt % Ru and 6 wt % Co) on alumina or silica support. The results show that combination of the two metals, both active in CO hydrogenation, gives a catalyst with 2 - 3 times higher activity on weight metal basis, than the two metals alone. The methane and olefin selectivity is lower and the higher hydrocarbon selectivity is higher for

the new catalyst system compared to both of the monometallic systems. The enhancement in activity is higher than the measured enhancement in the degree of reduction. This indicates that there are interactions between the two metals that modify their properties. Shpiro et al. found ruthenium-cobalt species. $RuCo^+$, in mass spectra investigations. From this they explain the synergistic action with bimetallic cluster formation and ligand effects giving increased CO dissociation on cobalt when modified with ruthenium. Increased hydrogen activation on ruthenium, activation of less reactive surface carbon species, and reduced formation of bulk oxide and carbide structures which may deactivate the catalyst, may also be linked to the increased activity /29/. This is in agreement with the suggestions of Guczi et al. /49/ from studies of CoIr catalysts.